

Total single-electron-capture cross sections for impact of H^+ , H_2^+ , He^+ , and Ne^+ (2–20 keV) on Li

Friedrich Aumayr and Hannspeter Winter

Institut für Allgemeine Physik, Technische Universität Wien, A-1040 Wien, Austria

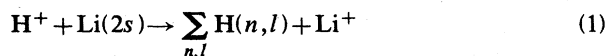
(Received 23 July 1984)

Total cross sections for single-electron capture from $Li(2s)$ by H^+ , H_2^+ , He^+ , and Ne^+ have been measured at impact energies between 2 and 20 keV. All data sets show maximum cross sections of about $5 \times 10^{-15} \text{ cm}^2$ and are compared with other available measurements as well as calculations.

I. INTRODUCTION

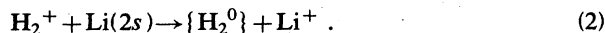
At comparably low impact velocities ($v < v_e$, the classical orbital velocity of the transfer electron prior to capture), electron capture from atoms by singly charged ions is most probable for channels with small reaction energy defects, i.e., quasis resonant reactions. With alkali-metal targets such quasis resonant reactions can proceed for singly ionized atom species, of which corresponding neutralized particles possess states with binding energies closely matching the alkali-metal-atom ionization potentials. Therefore, excited states of neutral atoms can be populated via electron capture from alkali-metal atoms with comparably large cross sections, which is of both fundamental and practical interest. In this context ion impact on Li corresponds to the most simple cases, but has been studied very little so far.

Recently, we have investigated state-selective electron capture and target excitation in inelastic H^+ -Li(2s) collisions.^{1,2} Consequently, cross sections σ_{10} for single-electron capture

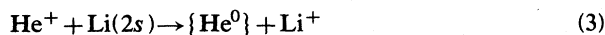


have now been determined at proton impact energies of 2–20 keV. The mentioned process has been theoretically studied^{3–6} by using either atomic or molecular expansions. Related experimental data are of interest for testing these calculations for reliability and accuracy. Furthermore, such processes are of interest for active neutral Li beam diagnostics^{7–9} of magnetically confined plasmas as discussed in Ref. 1.

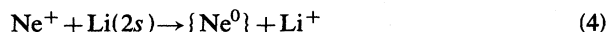
Previous measurements of σ_{10} for H^+ -Li are only accurate at proton impact energies up to 4 keV,¹⁰ but at higher impact energy they involve relatively large ($\geq 50\%$) errors.^{11,12} Moreover, Gruebler *et al.*¹² found significant differences in cross sections for collisions with deuterons and protons of the same velocity. To check whether this could have been caused by a H_2^+ admixture in the deuteron beam, we also measured cross sections for the process



Total single-electron-capture cross sections have also been measured for the reactions



and



at ion impact energies of 2–20 keV. The brackets $\{ \}$ indicate summation over all neutral states produced. For He^+ our data bridge a gap between recent results of Varghese *et al.*¹⁰ for impact energies up to 3 keV and data of McCullough *et al.*¹³ and Auciello *et al.*¹⁴ For Ne^+ the present data can only be compared with experimental results of Rille and Winter,¹⁵ which have been obtained with a different experimental approach.

II. EXPERIMENT

Total single-electron-capture cross sections σ_{10} have been measured with an experimental arrangement as outlined in Fig. 1. H^+ , H_2^+ , He^+ , or Ne^+ ions have been extracted from a Duoplasmatron ion source, accelerated to the required impact energy, focused by a magnetic quadrupole doublet, and charge-to-mass separated. The resulting nearly parallel ion beam was cleaned from neutrals or negative ions eventually formed by collisions with background gas particles (pressure typically less than 1×10^{-6} mbar) by means of parallel condensers and passed via a 1-mm-diameter aperture into the Li vapor cell. This resistively heated Li oven cell was made of pure soft iron. It had a length of 25 mm and entrance and exit apertures of 2- and 2.5-mm diameter, respectively. The intensity of the ion beam was not influenced when passing it through the empty target cell, as well as if the latter was heated up to its normal working temperature. Before making measurements, the filled Li oven was outgassed for typically one hour at a temperature substantially higher than at its operating conditions and was then allowed to reach thermal equilibrium at the required temperature. There, the fraction of Li dimers was probably less than 2%.¹⁶

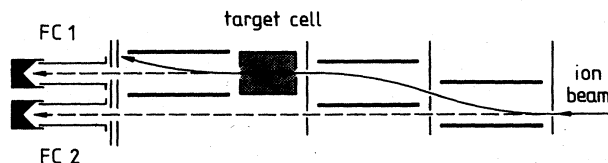


FIG. 1. Schematic view of experimental setup.

Behind the collision cell, the projectiles could be separated into ions and neutrals by means of deflection plates. With a Faraday cup (FC1) both the non-neutralized ions (deflection field off) and the neutralized atoms (deflection field on) could be registered via emission of secondary electrons. A second Faraday cup (FC2) served for monitoring the primary ion beam via fast neutral atoms produced by electron capture from background gas molecules prior to the collision region (cf. Fig. 1).

Under single-collision conditions (thin target) the fraction F_0 of neutralized projectiles is given by

$$F_0 = \frac{J_0}{J_1 + J_0} = 1 - \exp(-\sigma_{10}\Pi_{\text{Li}}) \simeq \sigma_{10}\Pi_{\text{Li}}, \quad (5)$$

where J_i denotes the flux of projectiles with charge i ($i=0$ or 1) and Π_{Li} is the Li target thickness. In Eq. (5) the quite improbable reactions of double-electron capture and stripping have been neglected. As mentioned before, the particle fluxes were determined by measuring secondary electron currents within a specially designed Faraday cup. It contained one electrode to stop the projectiles and another one biased by a positive potential of 60 V with respect to the former to catch all secondary electrons. For incident neutrals (deflection field on) the secondary electron current I can be expressed by

$$I^{(\text{on})} = \gamma_0 J_0 e \quad (6)$$

and for incident ions and neutrals (deflection field off) by

$$I^{(\text{off})} = \gamma_+ J_1 e + \gamma_0 J_0 e. \quad (7)$$

Here γ_+ and γ_0 denote the number of secondary electrons emitted per incident ion or neutral, respectively. While γ_+ could be easily measured, the coefficient γ_0 cannot be directly determined.

At low projectile velocities, secondary electron ejection is exclusively due to potential emission,¹⁷ which, however, is negligible for incident slow neutral atoms in their ground states. If the particle energy is raised above, typically, 100 eV/amu, kinetic emission sets in and toward higher impact energies will dominantly contribute to secondary electron production. Because an incident fast neutral atom is quickly stripped of its outermost electrons at the metal's surface, the kinetic emission is essentially independent of the charge state of the projectile.

Secondary emission coefficients for H^+ and H^0 impact have been measured for target materials such as gas-covered stainless steel,¹⁸ nickel,¹⁹ and copper beryllium.²⁰ From these investigations the following relation has emerged:

$$(\gamma_0/\gamma_+)_{\text{H}} = 1.11 + 0.001E(\text{keV}), \quad (8)$$

for a wide range of impact energies (1.6–55 keV), apparently independent of the target species and the angle of incidence.²¹ Accordingly, the neutral particles produce secondary electrons slightly more efficiently than singly charged ions of the same species and velocity, and the additional yield fraction is almost independent of the impact energy. These results have been explained²⁰ by assuming that for H^0 the electron bound to H^+ , which moves along with the incident proton, makes an extra contribution to

secondary electron production.

Corresponding measurements for the case of H_2^+/H_2 impact²⁰ have resulted in

$$(\gamma_0/\gamma_+)_{\text{H}_2} = 1.18 + 0.003E(\text{keV}) \quad (9)$$

and for impact of He^+ on He and Ne^+ on Ne have resulted in¹⁹

$$\gamma_{\text{He}^0} \simeq 1.05\gamma_{\text{He}^+} \quad (10)$$

and

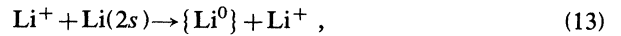
$$\gamma_{\text{Ne}^0} \simeq \gamma_{\text{Ne}^+}, \quad (11)$$

respectively. With this information, we could obtain the various F_0 by measuring the ratio of $I^{(\text{on})}$ and $I^{(\text{off})}$ and applying the relation

$$\frac{I^{(\text{on})}}{I^{(\text{off})}} = \frac{\gamma_0}{\gamma_+} \frac{J_0}{J_1 + \frac{\gamma_0}{\gamma_+} J_0} \simeq \frac{\gamma_0}{\gamma_+} \frac{J_0}{J_1 + J_0} = \frac{\gamma_0}{\gamma_+} F_0. \quad (12)$$

In all cases the fraction of ions undergoing charge exchange was less than 4%, so that the approximation in Eq. (12) remains accurate within 0.5%.

As a first step, the course of F_0 and thus of σ_{10} with impact energy was determined. In these measurements the stability of the Li target was checked by repeatedly taking data at 10 keV. The contribution to F_0 from collisions with the background gas, which could be measured by moving the Li target out of the ion beam, was always less than 5% and has been corrected for. To obtain absolute values for σ_{10} , the Li target thickness Π_{Li} had to be determined. Usually, this is achieved by measuring the target cell temperature and deriving the corresponding vapor pressure from data given in the literature. However, uncertainties among these data, which also deviate considerably from each other, contribute to the absolute error of σ_{10} . Additional errors arise from determination of the effective target length. We have circumvented these problems by comparing the fraction of neutralized projectiles F_0 to that resulting from the reference process



for which quite accurate cross sections ($\pm 15\%$) are known.²² They have been obtained by measuring the Li target thickness via surface ionization detection of Li atoms and taking into account the Li oven temperature.

The ratio of secondary electron emission coefficients for bombardment of targets such as Ag, Ta, Pt, Au, W, Be, Al, Ag-Mg, and Cu-Be by Li and Li^+ in the energy range 20–60 keV was found to be (cf. Ref. 23 and references therein)

$$(\gamma_0/\gamma_+)_{\text{Li}} = 1.1 \pm 10\%. \quad (14)$$

With this method, typical values for Π_{Li} in the order of $(4-8) \times 10^{12} \text{ cm}^{-2}$ have been obtained.

Finally, absolute data for σ_{10} have been obtained by comparing the fractions F_0 for Li and the ions of interest at the same Li target thickness. For this purpose, the primary ion species was changed from Li^+ to one of the projectile ions of interest and back in time intervals of typi-

TABLE I. Total single-electron-capture cross section for H^+ -Li collisions vs impact energy (total error: $\pm 20\%$).

Proton energy (keV)	σ_{10} (10^{-15} cm 2)
2	2.90
2.5	3.46
3	3.79
3.5	4.13
4	4.16
4.5	4.13
5	4.05
5.5	3.90
6	3.73
6.5	3.46
7	3.24
7.5	2.97
8	2.88
8.5	2.73
9	2.40
9.5	2.33
10	2.12
11	1.73
12	1.45
13	1.20
14	0.99
15	0.86
16	0.72
17	0.67
18	0.49
19	0.41
20	0.37

TABLE II. Total single-electron-capture cross sections for collisions of H_2^+ , $^4He^+$, and $^{20}Ne^+$ with Li vs impact energy (total error: $\pm 20\%$).

Projectile energy (keV)	σ_{10} (10^{-15} cm 2)		
	H_2^+ -Li	$^4He^+$ -Li	$^{20}Ne^+$ -Li
2	1.55	4.22	1.74
2.5		4.12	
3	2.44	4.12	2.16
3.5		4.49	
4	2.54	4.64	2.50
5	2.87	4.78	2.97
6	3.67	4.82	3.05
7	4.18	5.01	3.27
8	4.51	4.73	3.60
9	4.65	4.78	4.20
10	4.70	4.68	4.24
11	4.70	4.87	4.32
12	4.51	4.92	4.29
13	4.42	4.78	4.29
14	4.09	4.30	3.90
15	3.76	4.45	3.90
16	3.48	4.22	3.95
17	3.20	4.35	3.86
18	2.91	4.03	4.03
19	2.44	3.89	4.07
20	1.88	3.75	3.99

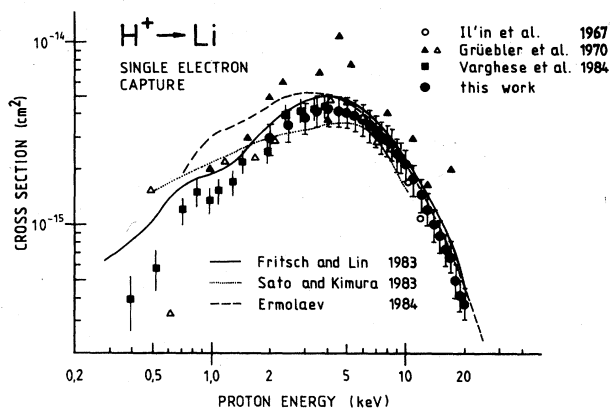


FIG. 2. Total single-electron-capture cross section for H^+ -Li collisions vs impact energy. Present data (full circles) are compared with other experiments (Refs. 10–12) and calculations (Refs. 4–6).

cally one minute, during which the Li target thickness apparently stayed constant. Therefore, total errors of our data result only from reproducibility over several individual sets of measurements (typically $\pm 4\%$), from errors for the used normalization cross sections ($\pm 15\%$), and for the ratios of secondary emission coefficients for neutrals and ions. Accordingly, the total error of our cross-section data is typically $\pm 20\%$.

III. RESULTS AND DISCUSSION

The measured cross sections σ_{10} are shown in Figs. 2–5 and listed in Tables I and II. All ion impact energies are given with respect to the laboratory system.

For H^+ -Li (Fig. 2) agreement with the recent experimental results of Varghese *et al.*¹⁰ in the overlapping energy region is excellent. Our data are also consistent with the previous results of Il'in *et al.*¹¹ The improvement in accuracy compared with the data of Gruebler *et al.*¹² is obvious. Comparison with available calculations shows that above 5 keV both the atomic-orbital (AO)– and

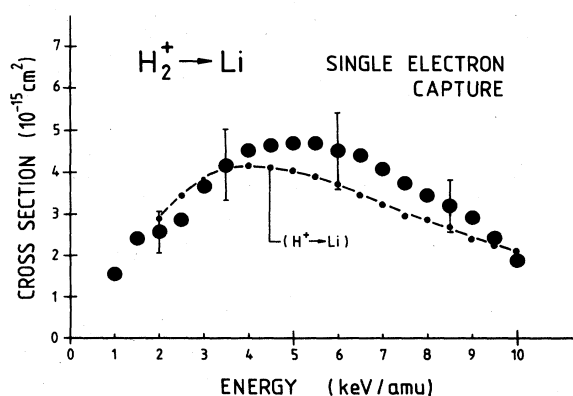


FIG. 3. Total single-electron-capture cross section for H_2^+ -Li collisions vs impact energy. Data are compared with cross sections for proton impact at the same velocity.

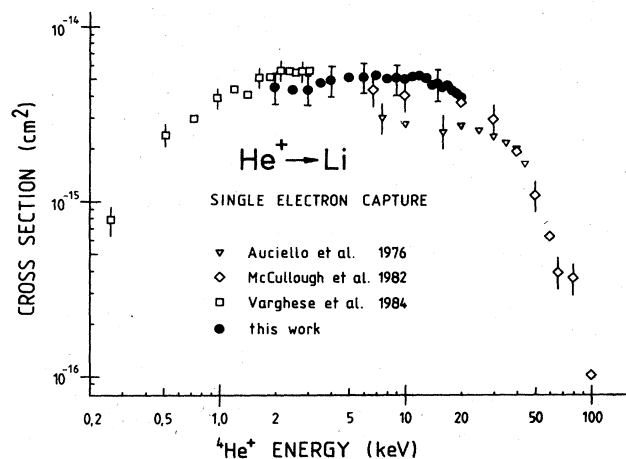


FIG. 4. Total single-electron-capture cross section for ${}^4\text{He}^+$ -Li collisions vs impact energy. Present data (full circles) are compared with other measurements (Refs. 10, 13, and 14).

molecular-orbital (MO) theories fit our experimental points well, but below 5 keV the atomic-orbital results of Ermolaev⁶ deviate significantly from the experimental data. The MO calculations of Allan *et al.*,³ which have not been shown in Fig. 2, consist of two separate sets of data depending on where the coordinate system has been fixed. Only below 6 keV do our data fall within these two curves. The AO+ calculations of Fritsch and Lin,⁴ which involve a modified atomic-orbital expansion method also including a number of united atom orbitals, represent the present data most satisfactorily.

In Fig. 3 our results for H_2^+ impact are compared with those for protons of the same velocity. Obviously, discrepancies in the data of Gruebler *et al.*,¹² as referred to in Sec. I, could not have been caused by H_2^+ impurities in the deuteron beam.

For He^+ -Li (Fig. 4) our data connect the results of Varghese *et al.*¹⁰ with those of McCullough *et al.*¹³ rather consistently, whereas the cross sections measured by Auciello *et al.*¹⁴ are about 40% smaller and also show a different energy dependence. We know of no calculations for this process.

In Fig. 5 our results for Ne^+ -Li are compared with data of Rille and Winter,¹⁵ which used the parallel plate condenser technique but the same normalization cross section for determination of the Li target thickness. Both sets of data agree well within their error limits. The σ_{10}

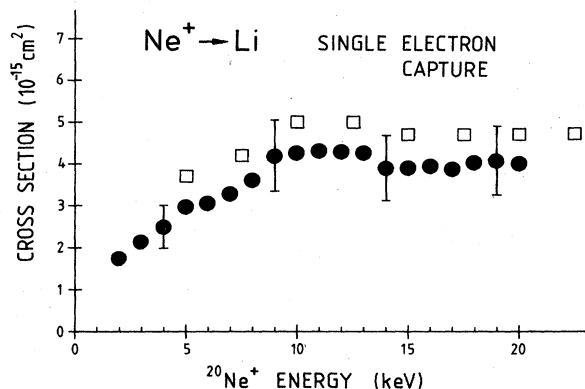


FIG. 5. Total single-electron-capture cross sections for ${}^{20}\text{Ne}^+$ -Li collisions vs impact energy. Present data (full circles) are compared with experimental results of Rille and Winter (Ref. 15, open squares).

versus impact-energy dependence shows a local maximum around 11 keV, which is probably due to contributions from the near-resonant capture into the $\text{NeI}(3s)$ states (cf. discussion in Ref. 15).

In conclusion, for all four collision systems investigated, we find cross-section maxima of typically $(4-5) \times 10^{-15} \text{ cm}^2$. The large size of these maxima is caused by electron capture into excited states of the neutral projectiles, which in all cases can take place with energy defects of less than 2 eV. The energy dependence of the cross sections can only be explained by state-selective studies, which so far have been made for the H^+ -Li system^{1,2} and, to a more limited extent, also for the Ne^+ -Li system.¹⁵

ACKNOWLEDGMENTS

This work has been supported by Austrian Fonds zur Förderung der Wissenschaftlichen Forschung (Projekt No. 4376), by Kommission zur Koordination der Kernfusionsforschung at the Austrian Academy of Sciences, and by International Atomic Energy Agency under Research Contract No. 2497/R4/RB. The authors are indebted to Mr. W. Beck and Mr. H. Schmidt for construction of the apparatus and to Mr. G. Lakits and Mr. C. Buchleitner for assistance during the measurements. Thanks are due to Dr. L. Cocke for advance information on data cited in Ref. 10.

¹F. Aumayr, M. Fehring, and H. Winter, *J. Phys. B* **17**, 4185 (1984).

²F. Aumayr, M. Fehring, and H. Winter, *J. Phys. B* **17**, 4201 (1984).

³R. J. Allan, A. S. Dickinson, and R. McCarroll, *J. Phys. B* **16**, 467 (1983).

⁴W. Fritsch and C. D. Lin, *J. Phys. B* **16**, 1595 (1983).

⁵H. Sato and M. Kimura, *Phys. Lett.* **96 A**, 286 (1983).

⁶A. M. Ermolaev, *J. Phys. B* **17**, 1069 (1984).

⁷H. Winter, *Comments At. Mol. Phys.* **12**, 165 (1982).

⁸K. McCormick, H. Murmann, M. El Shaer, and the ASDEX (Asymmetric Divertor Experiment) and NI (neutral-beam-injection) team, *J. Nucl. Mater.* **121**, 48 (1984).

⁹K. Kadota, K. Matsunaga, H. Iguchi, M. Fujiwara, K. Tsuchi-

- da, and J. Fujita, *Jpn. J. Appl. Phys.* **21**, L260 (1982).
- ¹⁰S. L. Varghese, W. Waggoner, and C. L. Cocke, *Phys. Rev. A* **29**, 2453 (1984).
- ¹¹R. N. Il'in, V. A. Oparin, E. S. Solov'ev, and N. V. Fedorenko, *Zh. Tekh. Fiz.* **36**, 1241 (1966) [*Sov. Phys.—Tech. Phys.* **11**, 921 (1967)].
- ¹²W. Gruebler, P. A. Schmelzbach, V. König, and P. Marmier, *Helv. Phys. Acta* **43**, 254 (1970).
- ¹³R. W. McCullough, T. V. Goffe, M. B. Shaw, M. Lennon, and H. B. Gilbody, *J. Phys. B* **15**, 111 (1982).
- ¹⁴O. Auciello, E. V. Alonso, and R. A. Baragiola, *Phys. Rev. A* **13**, 985 (1976).
- ¹⁵E. Rille and H. Winter, *J. Phys. B* **15**, 3489 (1982).
- ¹⁶R. J. Gordon, Y. T. Lee, and D. R. Herschbach, *J. Chem. Phys.* **54**, 2393 (1971).
- ¹⁷M. Kaminsky, *Atomic and Ionic Impact Phenomena on Metal Surfaces* (Springer, Berlin, 1965), Chap. 12.
- ¹⁸P. Pradel, F. Roussel, A. S. Schlachter, G. Spiess, and A. Valance, *Phys. Rev. A* **10**, 797 (1974).
- ¹⁹P. M. Stier, C. F. Barnett, and G. E. Evans, *Phys. Rev.* **96**, 973 (1954).
- ²⁰E. S. Chambers, *Phys. Rev.* **133**, A1202 (1964).
- ²¹C. F. Barnett and J. A. Ray, *Rev. Sci. Instrum.* **43**, 218 (1972).
- ²²J. Perel, H. L. Daley, J. M. Peek, and T. A. Green, *Phys. Rev. Lett.* **23**, 677 (1969).
- ²³G. Carter and J. S. Colligon, *Ion Bombardment of Solids* (Heinemann, London, 1968), p. 67.